Evaluation of the NCEP and MODIS Atmospheric Products for Single Channel Land Surface Temperature Retrieval With Ground Measurements: A Case Study of HJ-1B IRS Data

Hua Li, Qinhuo Liu, Yongming Du, Jinxiong Jiang, and Heshun Wang

***Abstract*—In this paper, two atmospheric profile sources were assessed for land surface temperature (LST) retrieval purposes for the HJ-1B IRS (Infrared Scanner) single-channel thermal infrared (TIR) data. One profile source is the National Center for Environmental Prediction (NCEP) operational global analysis data, and the other source is the Moderate Resolution Imaging Spectroradiometer (MODIS) atmospheric profiles product (MOD07). The atmospheric profiles were used as the input to the MODTRAN 4 radiative transfer model to calculate the atmospheric parameters involved in LST retrieval. The LST retrievals from the HJ-1B IRS data were compared with ground measured temperatures obtained from a series of field campaigns in Hebei province, China, from May to September of 2010. Ground measurements were performed over four land-cover types: bare soil, full-cover wheat, full-cover corn, and water surfaces. A total of 11 points of measurements was collected over a period of eight days. The results indicate that the LST derived from HJ-1B IRS data using either the NCEP or MOD07 profiles showed good agreement with the ground LSTs, with an root mean square error (RMSE) of 1.16 and 1.21 K for the NCEP and MOD07, respectively. In addition, we found that the MOD07 profiles may cause greater error for the atmospheric parameters estimation in the TIR domain for the regions of higher altitude due to a lack of data at the lower altitude levels. Thus, we proposed a method for combination of the MOD07 and NCEP profiles for LST retrieval. The results show that the combined profile is able to produce more reliable results than the use of only one type of profile because the combination offers both high spatial resolution and the necessary level of accuracy. This result implies that the combined profiles may be highly useful for accurate LST retrieval when local soundings are not available and particularly for sensors with only one thermal channel.**

***Index Terms*—Atmospheric profiles, HJ-1B IRS, land surface temperature (LST), MOD07, National Center for Environmental Prediction (NCEP).**

I. Introduction

To retrieve accurate geo/biophysical parameters from remote sensing data for earth observation applications, the effects of the atmosphere must be corrected in advance. In general terms, conversion from the top of atmosphere (TOA) signal to the ground-level signal is referred as atmospheric correction (AC) [1]. The main objective of AC in the thermal infrared (TIR) domain is retrieval of land surface temperature (LST) from the TOA radiance which is generally performed using the single-channel (SC) method or the split-window (SW) method [2]–[4]. To perform the single-channel method, an accurate radiative transfer model (RTM) such as MODTRAN 4 [5], and the relevant atmospheric profiles are acquired. The atmospheric profiles can generally be obtained by launching an atmospheric sounding near the time of the sensor overpass. However, local soundings are not available under most realistic conditions. Therefore, other sources of atmospheric profiles should be used in place of the sounding profiles. Currently, the atmospheric profiles can be obtained from satellite sounders or from the output of meteorological forecasting models, such as the Moderate Resolution Imaging Spectroradiometer (MODIS) atmospheric profile products (MOD07), the Atmospheric InfraRed Sounder (AIRS) atmospheric profile product, and the Global Data Assimilation System product provided by the National Centers for Environmental Prediction (NCEP) [6].

The NCEP profiles were first used in the standard atmospheric correction for ASTER TIR data to obtain the land-leaving radiance [7]. Subsequently, the NCEP profiles were gradually adopted for ACs of different satellite data, such as MODIS and Landsat TM/ETM+. Petitcolin *et al.* [8] used the NCEP profiles to perform an atmospheric correction of MODIS middle-thermal infrared radiances to retrieve land surface reflectance, emissivity and temperature in the middle and thermal infrared ranges. Barsi *et al.* [9] developed a web-based atmospheric correction tool (ACT) for the Landsat TM/ETM+ thermal band data. This tool uses the NCEP profiles (interpolated to a particular location, date and time) and the MODTRAN 4 model to calculate the atmospheric parameters. Barsi *et al.* [10] and Coll *et al.* [11] have demonstrated that this web-based ACT can provide LST estimates within an accuracy of ± 1 K for water surfaces and full-cover rice areas. Ellicott *et al.* [12] developed a parametric model for atmospheric correction in TIR for MODIS data, and the inputs of this model are the NCEP profiles. Li *et al.* [13] adapted this parametric model to the Chinese HJ-1B Infrared Scanner (IRS) data and used the NCEP profiles for retrieving LST from IRS data. Thus, the NCEP profiles have been used previously in many studies.

Manuscript received September 30, 2012; revised January 11, 2013 and February 25, 2013; accepted March 16, 2013. Date of publication April 11, 2013; date of current version June 17, 2013. This work was supported in part by Chinese Natural Science Foundation Project under Grant 41101325, National High Technology Research and Development Program of China under Grant 2012AA12A304, and Chinese Academy of Sciences/State Administration of Foreign Experts Affairs (CAS/SAFEA) International Partnership Program (KZZD-EW-TZ-09). *(Corresponding author: Q. Liu.)*

The authors are with the State Key Laboratory of Remote Sensing Science, Jointly Sponsored by the Institute of Remote Sensing and Digital Earth of Chinese Academy of Science and Beijing Normal University, Beijing 100101, China (e-mail: qhliu@irsa.ac.cn).

Digital Object Identifier 10.1109/JSTARS.2013.2255118

1939-1404/$31.00 © 2013 IEEE

Although the MOD07 is the existing atmospheric profile product with the highest spatial resolution, its use and validation have been relatively limited from 2000 to the present. The MOD07 products have been applied by different authors for estimation of clear-sky land surface upwelling longwave radiation and net radiation [14], [15]. Recently, Hulley & Hook [16] used the MOD07 profiles for generating consistent LST and emissivity products from ASTER and MODIS data with the Temperature Emissivity Separation (TES) algorithm [17].

In order to assess the accuracy of different profiles, several studies have been performed involving comparisons between different atmospheric profiles for AC and LST retrieval. Ellicott *et al.* [12] compared the AIRS and MODIS (MYD07) profile products with the Integrated Global Radiosonde Archive (IGRA) profiles for retrieving the LST from MODIS data. Their results indicate that the AIRS products demonstrate higher levels of accuracy than the MYD07 products for LST retrieval. Jiménez-Muñoz *et al.* [1] compared three different sources of atmospheric profiles with the local soundings for atmospheric correction in the optical region covering the visible and near infra-red (VNIR), short-wave infra-red (SWIR) and TIR regions. These profiles include the MOD07, the NCEP profiles from ACT, and the Modified Atmospheric Profiles from Reanalysis Information (MAPRI). The different sources of profiles were found to be useful for accurate ACs when the local soundings are not available. Coll *et al.* [18] compared four sources of atmospheric profiles for LST retrieval from single-channel TIR data, including radiosonde profiles, reanalysis profiles from the NCEP, and satellite retrieved profile products from the AIRS and MODIS. The results show that the radiosonde profiles provide the best results, the NCEP and MOD07 profiles yield reasonable results and the AIRS profiles provide the worst results, most likely due to their large temporal gap with the other satellite measurements.

As described above, one of the limitations for the SC method is a lack of local radiosonde profiles in most real cases [11]. Thus, the other sources of profiles offer alternatives to radiosonde data and provide a valuable means for spatializing the SC atmospheric correction at the regional scale, which is useful for operational generation of LST products from SC TIR data. However, the retrieval accuracy of the SC method depends largely on how well the atmospheric profiles represent the real state of the atmosphere over the studied area at the time of the satellite measurements [18]. Therefore, it is necessary to further assess the accuracy of the different profiles for LST retrieval from different sensor data. Thus, the objective of this paper is to assess the accuracy of the NCEP and MOD07 atmospheric profiles for LST retrieval using a comparison with concurrent ground LST measurements performed in China. The comparison focuses on the HJ-1B IRS (Infrared Scanner) single-channel TIR data with the aim of determining which type of profile is most suitable for generating LST product from HJ-1B IRS data.

Section II provides the theoretical basis for single-channel LST retrieval, a description of the NCEP and MOD07 atmospheric profiles, and the ground measurements and data used in this study. The results are presented and discussed in Section III, and the main conclusions of this study are summarized in Section IV.

TABLE I
SPECIFICATIONS OF THE HJ-1B MAIN PAYLOADS

Sensor	Band	Spectral range (μm)	Spatial resolution (m)	Swath width (km)	Field of view	Revisit time
CCD	1	0.43-0.52	30	360×2	31°	4 days
	2	0.52-0.60				
	3	0.63-0.69				
	4	0.76-0.9				
IRS	1	0.75-1.10	150	720	29°	4 days
	2	1.55-1.75				
	3	3.50-3.90				
	4	10.5-12.5	300			

II. METHODOLOGY

A. Theoretical Basis for Single-Channel LST Retrieval in the TIR

The satellite imagery used in this paper is the HJ-1B IRS data [13]. The HJ-1B satellite was launched on September 9, 2008, and is equipped with two CCD cameras and one IRS. Table I provides the specifications of the sensors onboard the HJ-1B. It should be noted that the IRS contains only one TIR channel. The most appropriate method to retrieve the LST from single-channel thermal data, as in the case of IRS, is by inversion of the radiative transfer equation (RTE) according to the following expression:

$$B_i(T_s) = \frac{L_i^{\text{sen}} - L_i^{\uparrow}}{\tau_i \varepsilon_i} - \frac{1-\varepsilon_i}{\varepsilon_i} L_i^{\downarrow} \tag{1}$$

$$T_s = \frac{c_2}{\lambda}\left[\ln\left(\frac{c_1}{\lambda^5 B_i(T_s)} + 1\right)\right]^{-1} \tag{2}$$

where $L_{\text{i}}^{\text{sen}}$ is the at-sensor radiance of channel i, T_s is the land surface temperature, $B_i(T_s)$ is the blackbody radiance of channel i, τ_i and ε_i are the atmospheric transmittance and land surface emissivity of channel i, $L_i^{\uparrow}$ is the atmospheric upwelling radiance of channel i, $L_i^{\downarrow}$ is the downwelling atmospheric irradiance divided by π, c_1 and c_2 are constants, with values of 1.19104×10^8 Wμm^{4}m^{-2}sr^{-1} and 14387.7 μmK, respectively, and λ is the wavelength.

The use of the central wavelength value in (2) for the LST inversion introduces a certain amount of error into T_s because the sensor is characterized by a certain channel width (referred to as bandpass effects) [19], [20]. Additional details on the bandpass effects can be found in [20]. To reduce these errors, we adapted a quadratic approximation for the Planck function.

Taking into account the spectral response function of the HJ-1B IRS TIR channel, the integrated channel radiance was calculated using

$$B_i(T_i) = \frac{\int_{\lambda_1}^{\lambda_2} B_\lambda(T_i) f(\lambda) d\lambda}{\int_{\lambda_1}^{\lambda_2} f(\lambda) d\lambda} \tag{3}$$

from 260 to 340 K in intervals of 1 K according to the normal range of the LST, where B_λ is the Planck function, T_i is the LST

in channel i, $f(\lambda)$ is the spectral response function, and λ_1 and λ_2 are the lower and upper wavelength boundaries, respectively.

The following quadratic expression was constructed between the channel radiance and T_s with $R^2 = 1$:

$$B_i(T_s) = 0.0004986T_s^2 - 0.1694T_s + 15.14. \quad (4)$$

By solving (4), T_s can be finally inverted, and the error of estimating T_s from

$$T_s = \frac{0.1694 + \sqrt{0.1694^2 - 4 \times 0.0004986 \times [15.14 - B_i(T_s)]}}{2 \times 0.0004986} \quad (5)$$

ranges from 0.01 to 0.15 K under the temperature range mentioned above.

B. Atmospheric Profiles

Here, we provide a brief description of the two atmospheric profile sources used in this paper. The first is the NCEP profile at a one degree spatial resolution, and the second is the MODIS MOD07 product at a spatial resolution of 5 × 5 1-km pixels. The atmospheric profiles extracted from the two sources were converted into the MODTRAN 4 format to compute three atmospheric parameters (transmittance, upwelling and downwelling radiance). In this study, minor atmospheric constituents were assigned to the mid-latitude summer (MLS) standard atmosphere included in MODTRAN 4, and were assumed as representative of the atmospheric conditions from May to September in China.

1) NCEP Profiles: The NCEP data used in this study are the NCEP final operational global analysis data in the GRIdded Binary (GRIB1) format.[1] This product is from the Global Data Assimilation System (GDAS), which continuously collects observational data from the Global Telecommunications System (GTS) and other sources for numerous analyses. The data are on a 1° × 1° longitude/latitude grid and generated globally every 6 h (0:00, 06:00, 12:00, 18:00 UTC). The extracted atmospheric profiles have 26 mandatory levels from 1000 to 10 hPa: 1000, 975, 950, 925, 900, 850, 800, 750, 700, 650, 600, 550, 500, 450, 400, 350, 300, 250, 200, 150, 100, 70 50, 30, 20, and 10 hPa. Other vertical atmospheric parameters include the geopotential height, the air temperature and the relative humidity.

We followed the method proposed by Barsi *et al.* [9] to extract the profiles from the NCEP data. Additionally, the surface elevation was also considered. First, the profiles were extracted from the four grid corners surrounding a specific location. The four corner profiles were interpolated for each time, and the overpass time profiles were also interpolated, resulting in a single profile according to the latitude and longitude of the location. Next, the profile was linearly interpolated according to the elevation of the location. If the surface elevation of the given location was lower than the altitude of the first level (1000 mb), the elevation interpolation was not performed. The overpass time of the HJ-1B satellite in our study area is approximately 03:00 UTC (11:00 local solar time), and thus, the NCEP data at 0:00 and 06:00 UTC were used. The interpolations in time and space are both linear.

2) MOD07 Profiles: The MODIS project provides many standard products for the scientific community, and the atmospheric profile products represent one of them, denoted as MOD07 or MYD07 if the Terra or Aqua platforms are used, respectively. In this study, we only use the MOD07 products collected from the Terra platform because its overpass time is close to that of the HJ-1B.

The MOD07 product consists of several parameters, which include the total ozone burden, the atmospheric stability, the temperature and moisture profiles, and the atmospheric water vapor. All of these parameters are produced day and night at a 5 × 5 1-km pixel resolution when at least nine observations are cloud-free, providing a total of 20 atmospheric levels from 1000 to 5 hPa which are 1000, 950, 920, 850, 780, 700, 620, 500, 400, 300, 250, 200, 150, 100, 70, 50, 30, 20, 10, and 5 hPa. The MODIS atmospheric profile algorithm is a statistical regression with the option for a subsequent non-linear physical retrieval. A detailed description of this algorithm can be found in the MODIS atmospheric profile retrieval Algorithm Theoretical Basis Documents (ATBD) [21] and from the MODIS Atmosphere website at http://modis-atmos.gsfc.nasa.gov/MOD07_L2/.

The MOD07 collection 5 products were downloaded from the Level 1 and Atmosphere Archive and Distribution System (LAADS) for the desired sites and dates of this study in an Hierarchical Data Format (HDF), which includes the atmospheric data at a 5 × 5 1-km pixel resolution. To obtain the atmospheric profiles of our ground measurement sites, the MOD07 products were processed using the MODIS Conversion Toolkit (MCTK) [22], which is an HDF file conversion and projection utility for all known MODIS data products. The atmospheric profiles were extracted for a single pixel centered at the latitude and longitude of our ground measurement sites. For a given pixel, the values of the air temperature, the dew point temperature and the geopotential height were extracted from the MOD07 for the 20 nominal pressure levels.

C. Ground Measurements and Data Processing

To assess the accuracy of the two sources of atmospheric profiles for retrieval of the LST from the HJ-1B IRS TIR data, we carried out a series of ground measurements in the Hebei province of China from May to September of 2010. Two field sites were chosen, one located in Huailai county (40°21′N, 115°46′E), and the other located in Baoding city (38°42′N, 115°23′E), the altitudes of these two sites are 480 and 30 m, respectively.

Ground measurements were only performed when the sky over the site was apparently cloud free and were collected over four land cover types: bare soil, full-cover wheat, full-cover corn, and water surfaces. A large lake is present at the Huailai site (Guanting Lake), and thus a temporary moored self-made buoy was constructed to measure the water surface skin temperature. An Apogee SI-111 precision infrared radiometer was installed on the buoy, which was approximately 1.5 m above the water surface and 2 m from the buoy body. The absolute accuracy, $\sigma(\mathrm{cal})$, of the radiometer is $\pm 0.2^\circ$C [23]. Skin temperature measurements were collected every 5 s, and the data were transmitted through a wireless sensor network [24]. Six days of measurements over the water surface and three days of ground measurements over land were collected in these two sites. Table II

[1][Online]. Available: http://rda.ucar.edu/datasets/ds083.2/

TABLE II
LIST OF DATES AND OVERPASS TIMES OF THE HJ-1B IRS AND MODIS

Case	Site	Date (month/day/year)	Land cover type	Overpass time (UTC)	
				HJ-1B IRS	Terra MODIS
1	Baoding	05/13/2010	Wheat	03:22	03:50
2	Huailai	05/01/2010	Bare soil	03:14	03:25
3		07/18/2010	Water	03:12	03:40
4		08/14/2010	Water	03:15	03:20
5		08/15/2010	Water	03:28	02:25
6		09/14/2010	Water	02:56	02:40
7			Water		
8		09/22/2010	Corn 1	03:01	03:25
9			Corn 2		
10			Corn 3		
11		09/26/2010	Water	03:04	03:00

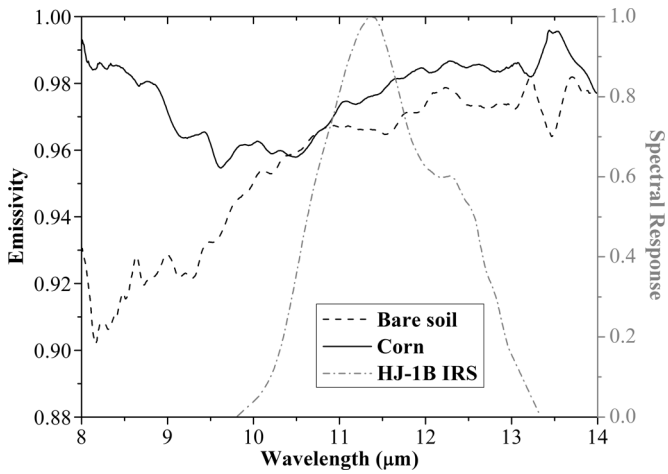

Fig. 1. Emissivity spectra of the measured bare soil and corn samples and the spectral response function of the HJ-1B IRS TIR channel.

presents a list of all dates and the overpass times of the HJ-1B IRS and MODIS data.

For the measurements collected over land, the ground temperatures were measured by person using several different broadband thermal radiometers (8–14 μm). The instruments include one FLUKE 66 radiometer, one RAYTEK ST60 radiometer, and three domestic IRTA-301AL precision infrared radiometers.[2] The designed accuracy of these radiometers is $\pm 1\%$ of reading or $\pm 1\ ^{\circ}$C. The Huailai site is a corn crop area and the Baoding site is a wheat crop area. The topography of two sites is notably flat and the crop areas of two sites are larger than 6 km^2 which are suitable for LST validation. One point of ground measurement for bare soil and three points for corn were obtained at the Huailai site on May 1, 2010, and September 22, 2010, respectively. Only one point of measurement for wheat was obtained at the Baoding site on May 13, 2010. The distance between three corn points at the Huailai site was greater than 400 m, which is larger than one IRS pixel size. During the field campaigns, the radiometers were carried back and forth along transects approximately 50 m long to observe the surface at view angles close to the nadir. The field of view of the radiometers was 30–50 cm on the soil/crop surface. Measurements were collected at a rate of greater than 20 per minute. The data were collected during periods of 15–20 min centered on the satellite overpass time. We recorded the time of the measurements and the corresponding radiometric temperatures for every minute. The measured temperature data were processed to obtain the real LSTs, which were subsequently compared with the satellite-derived LSTs. Following the study of Coll *et al.* [25], three different processes were applied.

1) Calibration: All of the radiometers were calibrated after each field campaign using a MIKRON M340 calibration blackbody within a temperature range from 0 °C to 60 °C within a step size of 5 °C. The absolute accuracy of the M340 blackbody is ± 0.3 K.[3] According to the calibration results, the accuracy for the radiometers ranged from ± 0.2 to ± 0.4 K after the calibration. Thus, the final calibration accuracy, $\sigma(\mathrm{cal})$, was between ± 0.4 and ± 0.5 K.

2) Emissivity Correction: The measured radiometric temperatures must be corrected for emissivity and the downward sky irradiance effect. If T_{r} is the radiometric temperature measured by a radiometer, the true LST T is given by [25]

$$B(T) = \frac{[B(T_{\mathrm{r}}) - (1-\varepsilon)L_{\mathrm{sky}}]}{\varepsilon} \tag{6}$$

where B is the Planck function weighted for the spectral response function of the radiometer, ε is the surface emissivity, and L_{sky} is the downward sky irradiance divided by π.

The emissivity measurements were performed with ABB BOMEM MR304 spectroradiometers and a diffuse golden plate, which were used to obtain the radiometric data of the samples and the corresponding atmospheric downward radiance. We measured the bare soil and corn samples in the field only after the ground measurements of the temperature. Three samples of each surface type were measured and three measurements were made consecutively for each sample. The spectral resolution of the MR304 is 1 cm^{-1}. The emissivity spectra in the range of 8–14 μm were retrieved using the Iterative Spectrally Smooth Temperature and Emissivity Separation (ISSTES) algorithm [26], which has been proven as an effective algorithm with high accuracy for temperature and emissivity retrieval [27], [28]. The retrieved emissivity spectra of the bare soil and corn samples and the spectral response function of the HJ-1B TIR channel are shown in Fig. 1. The uncertainty for the emissivity derived by the ISSTES algorithm is approximately 0.01 [28]. Emissivity values of 0.954 ± 0.005 and 0.976 ± 0.004 were obtained for the bare soil and corn at the Huailai site. *Coll et al.* [18] indicated that full-cover rice crops have uniform and high emissivity values ($\varepsilon = 0.983 \pm 0.005$) with small spectral variation in the range of 8–13 μm, and thus we use this emissivity value for the only full-cover wheat point at the Baoding site. For the water emissivity, we directly used the three water spectra in the ASTER spectral library [29]. The reflectance was converted to emissivity using Kirchhoff's law and subsequently convolved with the SI-111 spectral response function to obtain a channel value. Finally, a value of 0.983 was obtained for water.

Considering an emissivity uncertainty of ± 0.01, which is larger than the uncertainties in the emissivity values listed

[2][Online]. Available: http://www.irtc.com.cn/infra.htm

[3][Online]. Available: http://www.transcat.com

TABLE III
GROUND-MEASURED LSTS (CALIBRATED AND EMISSIVITY CORRECTED) AND CORRESPONDING UNCERTAINTIES

Case	Date	Land cover type	Ground LST (K)	σ(*T*) (K)
1	05/13/2010	Wheat	294.73	1.09
2	05/01/2010	Bare soil	312.54	1.33
3	07/18/2010	Water	298.08	0.49
4	08/14/2010	Water	297.16	0.50
5	08/15/2010	Water	298.32	0.98
6	09/14/2010	Water	296.92	0.61
7	09/22/2010	Water	290.32	0.45
8	09/22/2010	Corn 1	289.48	1.54
9	09/22/2010	Corn 2	292.08	1.49
10	09/22/2010	Corn 3	291.62	1.57
11	09/26/2010	Water	290.20	0.43

above, the emissivity correction errors $(\sigma(\mathrm{em}))$ range from ± 0.3 K to ± 0.5 K, depending on the magnitude of L_{sky} and the temperature range in this study.

3) Averaging of Ground Temperature for Each Point: In this study, we considered only temperatures measured within 2 minutes of the satellite overpass time. These data were averaged for each point and the standard deviation of the measured temperatures was calculated as the spatial/temporal variability of the LST in the test sites, $\sigma(\mathrm{var})$.

Therefore, the total uncertainty in the temperature measurement for each radiometer, $\sigma(T)$, is given by the combination of the three sources of error (calibration, emissivity correction, and spatial/temporal variability) [25], as follows:

$$\sigma(T) = \left[\sigma(\mathrm{cal})^2 + \sigma(\mathrm{em})^2 + \sigma(\mathrm{var})^2\right]^{\frac{1}{2}}. \tag{7}$$

Table III summarizes the ground-measured LSTs and the corresponding total uncertainties calculated by (7). Values of ± 1.3 K and ± 1.6 K were obtained for bare soil and corn, revealing a relatively high thermal homogeneity for the experimental fields, and $\sigma(\mathrm{var})$ was the largest source of error for bare soil and corn surfaces in our study. The water LSTs have lower uncertainties indicating that water is more homogeneous and more suitable for LST validation.

III. RESULTS AND DISCUSSION

A. Comparison of Profiles and Atmospheric Parameters

Prior to the comparison of the LST retrieval results, we directly compared the vertical information of the NCEP and MODIS atmospheric profiles. The air and dew point temperatures at different pressure levels for the two profiles on May 1, 2010 and May 13, 2010 were plotted in Fig. 2 for the two sites. The figure shows that the NCEP and MOD07 provide a similar air temperature shape, in particular for pressure levels between 1000 and 150 hPa. Large differences occur in the region between 150 and 50 hPa. Additionally, the differences for the Huailai site are smaller than those for the Baoding site. Notably large differences were found in the dew point temperature profiles. Large differences are observed at levels between approximately 800 and 500 hPa for the Huailai site, and 500 and 200 hPa for the Baoding site. In addition, there are no data for several top levels of the NCEP profile that have very low water vapor content, because the relative humidity profile only contains 21 levels from 1000 to 100 hPa for the NCEP data. We found that there were no data in the first three atmospheric levels of the MOD07 profile at the Huailai site, and the first pressure level was 850 hPa for all of the MOD07 profiles. However, the first pressure level of the NCEP profiles occurs at approximately 950 hPa for the Huailai site after interpolation of the elevation, according to the altitude of this site (480 m). At the Baoding site, the first pressure levels of the NCEP and MOD07 profiles both occur at 1000 hPa, because this site is located at a rather low altitude (30 m). This implies that the MOD07 profiles may contain less information than the NCEP profiles for the near-surface levels in the higher altitude areas.

The water vapor content (W) is a key atmospheric variable in the single-channel LST retrieval [30], because it is well correlated with the atmospheric transmittance and radiance. The water vapor contents were calculated from the NCEP and MOD07 profiles and are listed in Table IV for comparison. Note that four points of measurements (one water and three corn points) are listed on September 22, 2010, at the Huailai site that use the same atmospheric profiles due to the relatively low spatial resolution of the profiles. In general, the NCEP yielded larger W values than the MOD07, with differences up to 0.7 g/cm^2 at the Huailai site, except for the result of September 22, 2010. We checked the dew point temperature profiles of September 22, 2010, and found that the values for the NCEP were much lower than those of the MOD07 for levels between 1000 and 700 hPa, with differences of 6 K on average. Hence, the water vapor content was lower for the NCEP on September 22, 2010. Similar values were obtained at the Baoding site for the two profiles with a difference of 0.15 g/cm^2.

The three atmospheric parameters involved in the single channel LST retrieval are also listed in Table IV for comparison. It is worth mentioning that the MODTRAN provides the parameter $L^{\uparrow}$ for a given view angle as an output. A complete calculation of the reflection term requires the evaluation of $L^{\downarrow}$ at all view angles covering the hemisphere. In this study, the $L^{\downarrow}$ values at 53° were used in place of the hemispheric value [31].

It can be observed that the atmospheric transmittances calculated from the MOD07 profiles are much higher than those computed from the NCEP profiles for cases 2, 3, 4, 5, and 6 with differences up to 0.13 at the Huailai site, because the water vapor contents calculated from NCEP profiles are much higher for these cases and the atmospheric transmittance decreases linearly with W in general. In addition, the atmospheric transmittance of the NCEP is higher than that of the MOD07 for cases 7–10 (September 22, 2010) because the W for the NCEP is smaller, as described above. The atmospheric transmittances for the NCEP and MOD07 at the Baoding site (case 1) exhibit the same value because the water vapor content values are quite close for the two profiles. The atmospheric radiances show the same variation when compared with the atmospheric transmittances. The results of the NCEP are higher than those of MOD07 for cases 2, 3, 4, 5, 6, and 8 at the Huailai site. Similarly, the atmospheric radiances calculated from the two profiles at the Baoding site (case 1) are very close. Therefore, the MOD07 profiles may provide an overestimation of the atmospheric transmittance due

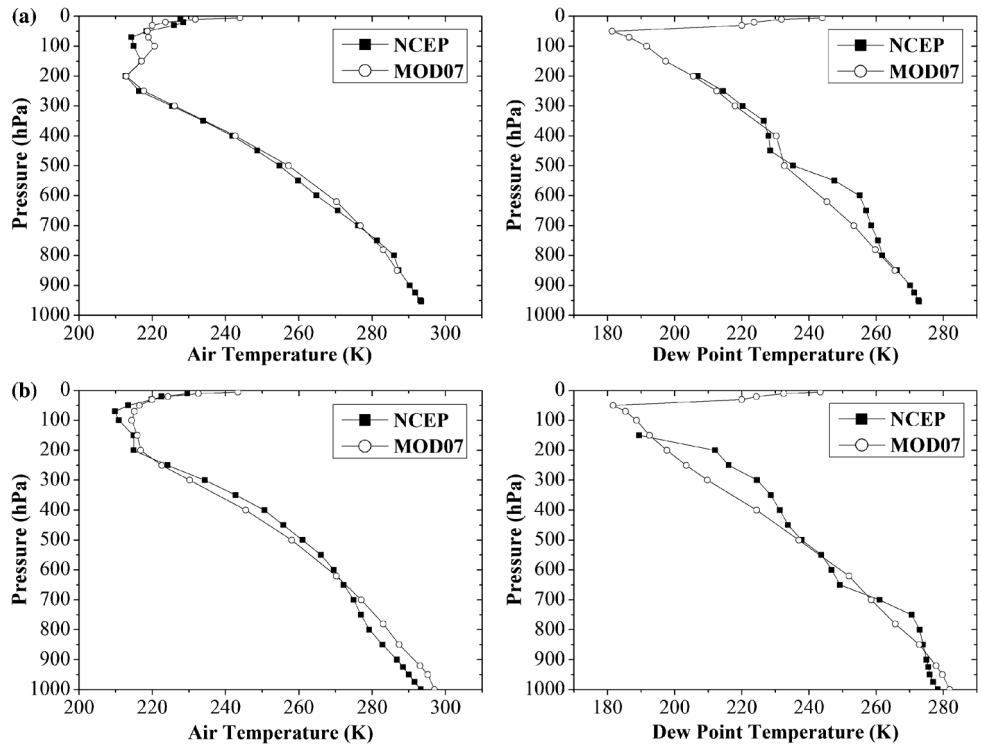

Fig. 2. Vertical distribution of the air (left column) and dew point (right column) temperatures of the NCEP and MOD07 profiles in two test sites on (a) 1st May 2010 for the Huailai site and (b) 13th May 2010 for the Baoding site.

TABLE IV
ATMOSPHERIC PARAMETERS CALCULATED FROM THE NCEP AND MOD07 ATMOSPHERIC PROFILES (W:g/cm^2, L : Wm^{-2}sr$^{-1}\mu$m^{-1})

Case	Date	NCEP				MOD07			
		W	τ	$L^{\uparrow}$	$L^{\downarrow}$	W	τ	$L^{\uparrow}$	$L^{\downarrow}$
1	05/13/2010	1.61	0.78	1.64	2.47	1.76	0.78	1.70	2.63
2	05/01/2010	0.96	0.88	0.87	1.36	0.63	0.92	0.48	0.79
3	07/18/2010	2.19	0.74	2.04	3.14	1.70	0.82	1.39	2.20
4	08/14/2010	1.75	0.79	1.52	2.37	1.66	0.82	1.37	2.17
5	08/15/2010	2.27	0.71	2.19	3.33	1.66	0.81	1.37	2.16
6	09/14/2010	2.14	0.72	2.17	3.30	1.40	0.85	1.13	1.80
7-10	09/22/2010	0.88	0.88	0.78	1.22	1.20	0.85	0.98	1.55
11	09/26/2010	0.75	0.90	0.64	1.00	0.78	0.91	0.53	0.84

to the lack of information from the lower altitude levels in the higher altitude region, thus yielding an underestimation of the atmospheric radiances, which may cause greater errors for atmospheric correction in the TIR domain.

B. Comparison of the LST Results

In order to further assess the accuracy of these two atmospheric profiles for LST retrieval from the HJ-1B IRS data, we followed the methodology described in Section II to obtain the corresponding satellite-derived LSTs using (1) and (5). The field measured and ASTER spectral library emissivity curves were converted to the HJ-1B IRS TIR channel emissivity using the IRS spectral response function. Different emissivity values were obtained: 0.967 for bare soil, 0.977 for full-cover corn, 0.983 for full-cover wheat, and 0.987 for water surfaces. In order to reduce the error caused by image geometric registration or surface heterogeneity, we also calculated the mean value of 3 × 3 pixels centered on the measured point. The results of the comparison between the ground LSTs and the HJ-1B IRS LSTs derived from the two sources of atmospheric profiles are shown in Table V.

The LST results derived from the two profiles both showed good agreement with the ground LSTs and the NCEP profiles obtained a slightly higher accuracy for the RMSE results. The NCEP profiles have an average bias of 0.29 K and an RMSE of 1.09 K for the 1-pixel case. The MOD07 profiles have an average bias of 0.12 K and an RMSE of 1.22 K. The low RMSE results indicate that the NCEP and MOD07 profiles are both valid for retrieving LSTs from IRS TIR data at the validation site. The 3 × 3 pixel average LSTs also agree well with the ground LSTs, and no large differences are observed from the 1-pixel results. The differences between the two results are smaller than 0.4 K for Huailai site and equal to 0.82 K for the BaoDing site. This result indicates that the validation sites are homogeneous at the 300 m scale and can be used for HJ-1B IRS LST validation in the future. In addition, our results are consistent with the study of Coll *et al.* [18], who compared the NCEP and MOD07 profiles for LST retrieval from Landsat ETM+ single channel thermal data in a homogeneous rice area and found that the two profiles yield similar results, with RMSE values of approximately 1 K. In addition, the water surface produced the best results, which was consistent with the results of Barsi *et al.* [10]

As described in the previous subsection, the MOD07 profiles underestimated the water vapor content due to a lack of information on the lower altitude levels which may cause errors in the LST retrieval. Thus, this effect was analyzed further. The LST

TABLE V
COMPARISON OF GROUND AND IRS LSTS DERIVED FROM THE NCEP AND MOD07 PROFILES

Case	Date	Land cover type	NCEP				MOD07			
			IRS LST (K)		IRS-Ground LST (K)		IRS LST (K)		IRS-Ground LST (K)	
			1 pixel	3×3pixel	1 pixel	3×3 pixel	1 pixel	3×3pixel	1 pixel	3×3 pixel
1	05/13/2010	Wheat	294.92	295.74	0.19	1.01	294.27	295.09	-0.46	0.36
2	05/01/2010	Bare soil	311.32	310.95	-1.22	-1.59	311.24	310.89	-1.3	-1.65
3	07/18/2010	Water	298.79	298.60	0.71	0.52	298.24	298.06	0.16	-0.02
4	08/14/2010	Water	298.60	298.86	1.44	1.7	297.48	297.73	0.32	0.57
5	08/15/2010	Water	297.15	297.46	-1.17	-0.86	296.72	297.00	-1.6	-1.32
6	09/14/2010	Water	296.40	296.48	-0.52	-0.44	295.74	295.81	-1.18	-1.11
7	09/22/2010	Water	290.98	291.12	0.66	0.8	291.33	291.47	1.01	1.15
8	09/22/2010	Corn 1	291.87	291.77	2.39	2.29	292.21	292.10	2.73	2.62
9	09/22/2010	Corn 2	291.56	291.65	-0.52	-0.43	291.88	291.97	-0.2	-0.11
10	09/22/2010	Corn 3	291.87	291.72	0.25	0.1	292.21	292.05	0.59	0.43
11	09/26/2010	Water	291.13	291.20	0.93	1	291.42	291.49	1.22	1.29
		Bias (K)			0.29	0.37			0.12	0.20
		Standard deviation (K)			1.10	1.15			1.27	1.26
		RMSE (K)			1.09	1.16			1.22	1.21

differences calculated from the two profiles for the 3 × 3 pixel case and the W from the NCEP profiles are plotted in Fig. 3. It can be observed that the LST differences are higher for cases 1, 3, 4, 5, and 6 with differences up to 1.12 K, and lower for case 2 and cases 7–11, with differences up to 0.35 K. It should be noted that the large differences found in the atmospheric parameters calculated from the two profiles (see Table IV) are not reflected in the LST retrievals for case 2, perhaps because the magnitudes of the atmospheric parameters for case 2 are rather small. In contrast, the small differences in the atmospheric parameters can cause large LST differences for case 1 because the magnitudes of the atmospheric parameters are also large. It can be concluded that the NCEP and MOD07 profiles provide similar LST retrieval results when the water vapor content is lower than 1 g/cm^2, such as case 2 and cases 7–11. When the water vapor content is higher than 1.6 g/m^2, the LSTs retrieved from the two profiles display larger differences, such as cases 1, 3, 4, 5, and 6. In addition, the MOD07 profiles produced a higher accuracy for cases 1, 3, 4, and 9, but the NCEP profiles produced higher accuracy for cases 5, 6, 7, 8, 10, and 11. Because we only have 11 points for comparison, it is difficult to determine which profile is more accurate for single channel LST retrieval in general.

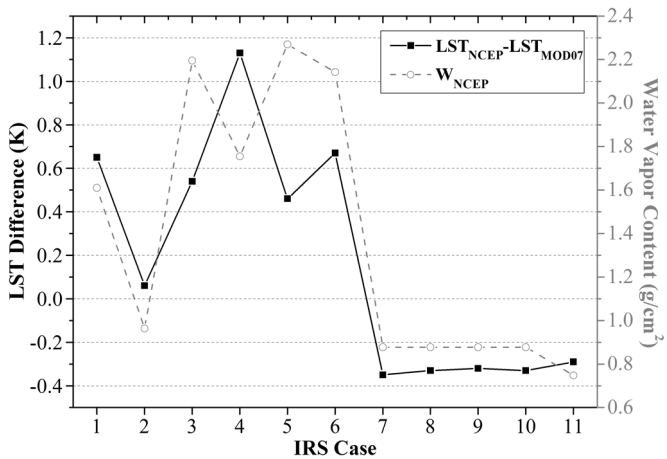

Fig. 3. LST differences between IRS-derived LSTs from the NCEP and MOD07 profiles and water vapor contents of the NCEP profiles.

In order to further analyze the altitude effect on the LST retrieval, we used the MODTRAN 4 to perform the simulation analysis. Four built-in standard atmospheric profiles were chosen for the analysis: the mid-latitude summer (MLS), sub-Arctic summer (SAS), mid-latitude winter (MLW) and sub-Arctic winter (SAW). The water vapor contents of these four profiles were 2.92, 2.08, 0.85, and 0.42 g/cm^2, respectively, which represents different levels of humidity. We assume that the real altitude of land surface is 0 km, the land surface emissivity is 0.98, the simulated LST ($T_{\text{simulated}}$) is 310 K, and the TOA radiance can subsequently be simulated using the MODTRAN 4 model for these four profiles. Next, changing the altitude of the four profiles from 0 to 3 km in steps of 0.2 km, and, assuming this value as the altitude error, the atmospheric parameters of different altitudes were calculated using MODTRAN 4. The LST was retrieved using the atmospheric parameters of different altitudes from the same simulated TOA radiance. The LST errors between the retrieved LST ($T_{\text{retrieved}}$) and the simulated LST for different altitudes are plotted in Fig. 4. This figure shows that the LST errors

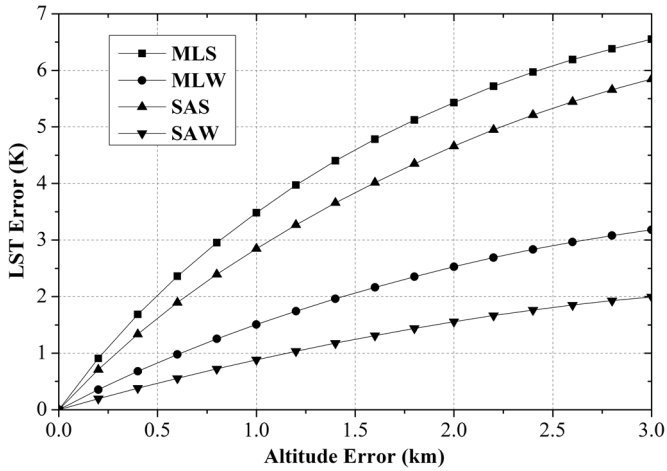

Fig. 4. Error in LST as a function of the altitude error for four standard atmospheric profiles.

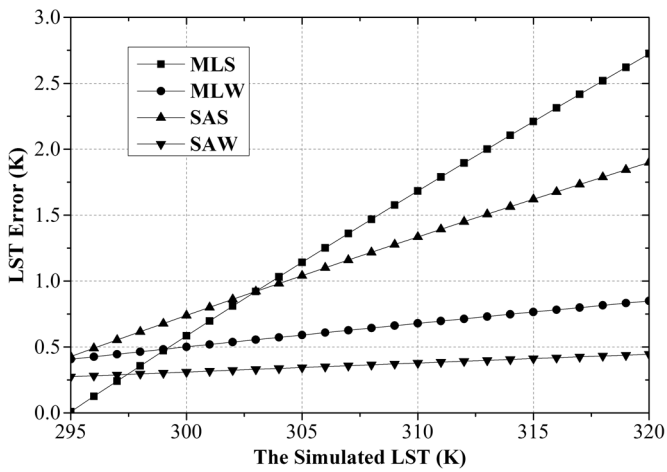

Fig. 5. Error in land surface temperature as a function of the simulated LST for four standard atmospheric profiles. An error of 0.6 km for surface elevation was assumed.

increase with the surface elevation error, and the profile with a higher water vapor content contains a larger error because the errors of the atmospheric parameters are increasing with the surface elevation and water vapor content.

Because we have LST results for different ranges, we also performed another analysis to reveal the LST error changes in different temperature ranges for the four profiles. During simulation of the TOA radiance, the simulated LST was changed from 295 to 320 K in steps of 1 K. Generally, the LST is higher than the air temperature of the first level, such that the minimum temperature is 295 K. Next, we assume the surface elevation error is 0.6 km for the LST retrieval. Thus, the atmospheric parameters of the 0.6 km altitude were used to retrieve the LST and subsequently compared with the simulated LST. Fig. 5 shows the error in the LST for different temperature values when the surface elevation error is 0.6 km for the four profiles. The LST errors are observed to increase rapidly with the increase in temperature for profiles with higher water vapor contents, such as the MLS and SAS profiles. In contrast, the LST errors increased slowly for the other two profiles with a low water vapor content,

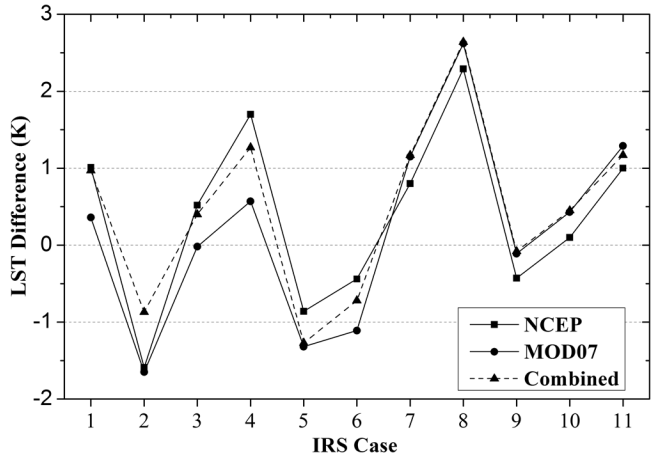

Fig. 6. LST differences between ground-measured and IRS-derived LSTs using different atmospheric profiles.

with errors smaller than 0.5 K between 295 and 320 K. This result indicates that the profiles with high humidity are more sensitive to the altitude error for the LST retrieval, which is consistent with the results described above (such as the LSTs retrieved from the NCEP and MOD07 profiles with higher differences for cases with a water vapor content higher than 1.6 g/cm^2 or quite close for water vapor contents lower than 1 g/cm^2).

C. Combination of the NCEP and MOD07 Profiles for LST Retrieval

The MOD07 product provides atmospheric information at the higher spatial resolution, but also provides less vertical information because it contains only 20 levels. In addition, this product offers fewer levels for regions with higher altitudes, such as the Huailai site in this study. The advantage that the NCEP offers over the MOD07 is greater vertical detail of the atmosphere, but this advantage is offset by the lower spatial resolution. Thus, a combination of the MODIS spatial and NCEP vertical resolutions may offer greater detail for the real atmospheric conditions.

The NCEP profiles contain more levels than the MOD07 in our validation sites, such as NCEP profiles have 25 levels and the MOD07 profiles only have 17 levels at the Huailai site. Hence, we assume that the NCEP profiles are more reasonable and more accurate for the real atmospheric conditions in terms of single channel LST retrieval. First, the MOD07 air temperature and dew point temperature values at each level were interpolated to the NCEP pressure levels using linear interpolation. Next, the air temperature and dew point temperature values of each level of the MOD07 and NCEP were averaged, but only the NCEP data were used for the levels for which the MOD07 contains no data. Thus, the new profiles were generated for the validation sites. Next, these profiles were used to calculate the atmospheric parameters and retrieve the LSTs. The results of the comparison between the retrieved LSTs and the ground LSTs for the 3×3 pixel case are shown in Fig. 6.

The LST results derived from the combined profiles also showed good agreement with the ground LSTs, with an average bias of 0.47 K and an RMSE of 1.19 K for the 3×3 pixel case. The results were improved for cases 2, 3, 4, and 9 when compared with the results of the NCEP and for cases 2, 5, 6,

and 11 when compared with the results of the MOD07, particularly for case 2, which was better than the results of both the NCEP and MOD07. In addition, the combined profiles obtained similar results when compared with the results of the NCEP or MOD07 for the other cases. This result implies that the combined profiles may provide more reliable results than the use of only one type of profile for single channel LST retrieval. Thus, merging the two profiles together could provide more stable results for the HJ-1B IRS LST product generation in high-altitude areas because it can provide atmospheric profiles with both high spatial resolution and the necessary level of accuracy. However, because we do not have enough validation points, a statistically significant conclusion with respect to the accuracy of the combined profiles cannot be drawn at this point, but will be the subject of further data collection and analysis in the future.

IV. Conclusion

The study reported in this paper assessed the accuracy of two atmospheric profile sources for deriving LSTs from the HJ-1B IRS TIR data: the NCEP operational global analysis data and the MODIS atmospheric profiles product (MOD07). The LSTs derived from the HJ-1B IRS TIR data after atmospheric correction using the NCEP and MOD07 data were compared with the ground-measured temperatures obtained from a series of field campaigns in Hebei province, China, from May to September of 2010. Ground measurements were performed over four land cover types: bare soil, full-cover wheat, full-cover corn, and water surface. A total of 11 points of measurements were collected over a period of eight days for the validation.

The results indicate that the LST derived from the HJ-1B IRS data using the NCEP and MOD07 profiles showed good agreement with the ground LSTs, and the NCEP profiles achieved a slightly higher accuracy than that of the MOD07 profiles for the RMSE results. This result means that these two atmospheric profile sources are both useful for LST retrieval if local soundings are not available, particularly for sensors with only one thermal channel.

In addition, we found that the MOD07 profiles may result in greater error for atmospheric parameters estimation in the TIR domain for regions with higher altitude due to the lack of data at the lower altitude levels. The main advantages of the MOD07 and NCEP profiles are the high spatial resolution and high vertical resolution, respectively. Thus, we proposed a method to combine the MOD07 and NCEP profiles together for the LST retrieval. The results indicate that the combined profiles are able to obtain more reliable results than the use of only one type of profile. Thus, merging the two profiles together may provide an approach that delivers a more stable HJ-1B IRS LST product for high-altitude areas because it can provide atmospheric profiles with both high spatial resolution and the necessary level of accuracy. Note that one limitation of this study is that the validation points are small in number, and we intend to collect additional ground LST measurements to further validate the accuracy of the different profiles for LST retrieval from IRS data in future research, particularly for regions of high altitude. Finally, the results presented in this paper refer to small areas with midlatitude summer conditions, and further analysis is required for additional areas and atmospheric conditions.

Acknowledgment

The authors would like to thank anonymous referees for their comments and suggestions that have significantly improved the article. The authors would also like to thank Dr. J. Barsi for the discussion about the NCEP data and Dr. H. Wu for help revising the paper. The NCEP data for this study are from the Research Data Archive (RDA) which is maintained by the Computational and Information Systems Laboratory (CISL) at the National Center for Atmospheric Research (NCAR). NCAR is sponsored by the National Science Foundation (NSF). The original data are available from the RDA[4] in dataset number ds083.2. MODIS MOD07 products were obtained through NASA's Goddard Space Flight Center LAADS web. The authors would also like to thank the people who carried out the ground measurements.

References

[1] J. C. Jiménez-Muñoz, J. A. Sobrino, C. Mattar, and B. Franch, "Atmospheric correction of optical imagery from MODIS and Reanalysis atmospheric products," *Remote Sens. Environ.*, vol. 114, pp. 2195–2210, 2010.

[2] J. C. Jiménez-Muñoz, J. Cristobal, J. A. Sobrino, G. Soria, M. Ninyerola, and X. Pons, "Revision of the single-channel algorithm for land surface temperature retrieval from Landsat thermal-infrared data," *IEEE Trans. Geosci. Remote Sens.*, vol. 47, no. 1, pp. 339–349, Jan. 2009.

[3] Z.-L. Li, B.-H. Tang, H. Wu, H. Z. Ren, G. J. Yan, Z. Wan, I. F. Triggo, and J. A. Sobrino, "Satellite-derived land surface temperature: Current status and perspectives," *Remote Sens. Enviro.*, vol. 131, pp. 14–37, Apr. 2013.

[4] Z.-L. Li, H. Wu, N. Wang, S. Qiu, J. A. Sobrino, Z. Wan, B.-H. Tang, and G. J. Yan, "Land surface emissivity retrieval from satellite data," *Int. J. Remote Sens.*, vol. 34, no. 9–10, pp. 3084–3127, 2013.

[5] A. Berk, G. P. Anderson, P. K. Acharya, J. H. Chetwynd, L. S. Bernstein, E. P. Shettle, M. W. Matthew, and S. M. Adler-Golden, *MODTRAN 4 User's Manual*. Hanscom AFB, MA, USA: Air Force Res. Lab., 1999.

[6] E. Kalnay, M. Kanamitsu, R. Kistler, W. Collins, D. Deaven, L. Gandin, M. Iredell, S. Saha, G. White, J. Woollen, Y. Zhu, M. Chelliah, W. Ebissuzaki, W. Higgins, J. Janowiak, K. C. Mo, C. Ropelewski, J. Wang, A. Leetmaa, R. Reynolds, R. Jenne, and D. Joseph, "The NCEP/NCAR 40 year reanalysis project," *Bull. Amer. Meteorol. Soc.*, vol. 77, no. 3, pp. 437–471, Mar. 1996.

[7] F. Palluconi, G. Hoover, R. Alley, M. J. Nilsen, and T. Thompson, "An atmospheric correction method for ASTER thermal radiometry over land," Algorithm Theoretical Basis Document Revision 3, Jet Propulsion Lab.. Pasadena, CA, USA, 1999.

[8] F. Petitcolin and E. Vermote, "Land surface reflectance, emissivity and temperature from MODIS middle and thermal infrared data," *Remote Sens. Environ.*, vol. 83, pp. 112–134, Nov. 2002.

[9] J. A. Barsi, J. L. Barker, and J. R. Schott, "An atmospheric correction parameter calculator for a single thermal band earth-sensing instrument," in *Proc. IEEE IGARSS*, Toulouse, France, 2003, pp. 3014–3016.

[10] J. A. Barsi, J. R. Schott, F. D. Palluconi, and S. J. Hook, "Validation of a web-based atmospheric correction tool for single thermal band instruments," in *Proc. SPIE*, 2005, vol. 5882, pp. 588 20E.1–588 20E.7.

[11] C. Coll, J. M. Galve, J. M. Sánchez, and V. Caselles, "Validation of landsat-7/ETM+ thermal-band calibration and atmospheric correction with ground-based measurements," *IEEE Trans. Geosci. Remote Sens.*, vol. 48, pp. 547–555, 2010.

[12] E. Ellicott, E. Vermote, F. Petitcolin, and S. J. Hook, "Validation of a new parametric model for atmospheric correction of thermal infrared data," *IEEE Trans. Geoscience and Remote Sensing*, vol. 47, no. 1, pp. 295–311, Jan. 2009.

[13] H. Li, Q. H. Liu, B. Zhong, Y. M. Du, H. S. Wang, and Q. Wang, "A single-channel algorithm for land surface temperature retrieval from HJ-1B/IRS data based on a parametric model," in *Proc. IEEE IGARSS*, Honolulu, HI, USA, 2010, pp. 2448–2451.

[4][Online]. Available: http://rda.ucar.edu

[14] G. Bisht, V. Venturini, S. Islam, and L. Jiang, "Estimation of the net radiation using MODIS (Moderate Resolution Imaging Spectro radiometer) data for clear sky days," *Remote Sens. Environ.*, vol. 97, no. 1, pp. 52–67, 2005.
[15] W. H. Wang and S. L. Liang, "Estimation of high-spatial resolution clear-sky longwave downward and net radiation over land surfaces from MODIS data," *Remote Sens. Environ.*, vol. 113, no. 4, pp. 745–754, 2009.
[16] G. C. Hulley and S. J. Hook, "Generating consistent land surface temperature and emissivity products between ASTER and MODIS data for earth science research," *IEEE Trans. Geosci. Remote Sens.*, vol. 49, no. 4, pp. 1304–1315, Apr. 2011.
[17] A. Gillespie, S. Rokugawa, T. Matsunaga, J. S. Cothern, S. Hook, and A. B. Kahle, "A temperature and emissivity separation algorithm for Advanced Spaceborne Thermal Emission and Reflection Radiometer (ASTER) images," *IEEE Trans. Geosci. Remote Sens.*, vol. 36, no. 4, pp. 1113–1126, Jul. 1998.
[18] C. Coll, V. Caselles, E. Valor, and R. Niclòs, "Comparison between different sources of atmospheric profiles for land surface temperature retrieval from single channel thermal infrared data," *Remote Sens. Environ.*, vol. 117, pp. 199–210, Feb. 2012.
[19] A. C. T. Pinheiro, J. Descloitres, J. L. Privette, J. Susskind, L. Iredell, and J. Schmaltz, "Near-real time retrievals of land surface temperature within the MODIS rapid response system," *Remote Sens. Environ.*, vol. 106, no. 3, pp. 326–336, Feb. 2007.
[20] R. Richter and C. Coll, "Band-pass resampling effects for the retrieval of surface emissivity," *Appl. Opt.*, vol. 41, no. 18, pp. 3523–3529, Jun. 2002.
[21] S. W. Seemann, E. E. Borbas, J. Li, W. P. Menzel, and L. E. Gumley, *MODIS Atmospheric Profile Retrieval Algorithm Theoretical Basis Document*. Madison, WI, USA: Univ. Wisconsin-Madison, 2006.
[22] [Online]. Available: http://www.exelisvis.com/Default.aspx?tabid=1540&id=1193
[23] [Online]. Available: http://www.apogeeinstruments.com/infraredradiometer/evaluating.html
[24] X. Li, X. Cheng, P. Gong, and K. Yan, "Design and implementation of a wireless sensor network-based remote water-level monitoring system," *Sensors*, vol. 11, no. 2, pp. 1706–1720, Feb. 2011.
[25] C. Coll, V. Caselles, J. M. Galve, E. Valor, R. Niclòs, J. M. Sánchez, and R. Rivas, "Ground measurements for the validation of land surface temperatures erived from AATSR andMODIS data," *Remote Sens. Environ.*, vol. 97, no. 3, pp. 288–300, Aug. 2005.
[26] C. C. Borel, "Surface emissivity and temperature retrieval for a hyperspectral sensor," in *Proc. IEEE IGARSS*, 1998, vol. 1, pp. 546–549.
[27] P. M. Ingram and A. H. Muse, "Sensitivity of iterative spectrally smooth temperature/emissivity separation to algorithmic assumptions and measurement noise," *IEEE Trans. Geosci. Remote Sens.*, vol. 39, no. 10, pp. 2158–167, Oct. 2001.
[28] J. Cheng, S. Liang, J. Wang, and X. Li, "A stepwise refining algorithm of temperature and emissivity separation for hyperspectral thermal infrared data," *IEEE Trans. Geosci. Remote Sens.*, vol. 48, no. 3, pp. 1588–1597, Mar. 2010.
[29] A. M. Baldridge, S. J. Hook, C. I. Grove, and G. Rivera, "The ASTER spectral library version 2.0," *Remote Sens. Environ.*, vol. 113, no. 4, pp. 711–715, April 15, 2009.
[30] J. C. Jiménez-Muñoz and J. A. Sobrino, "A generalized single-channel method for retrieving land surface temperature from remote sensing data," *J. Geophys. Res.*, vol. 108, no. D22, p. 4688, Nov. 2003, 10.1029/2003JD003480.
[31] K. Y. A. Kondratiev, "Radiation in the atmosphere," in *International Geophysics Series*. New York, NY, USA: Academic, 1969, vol. 12, p. 911.

Hua Li received the B.Sc. degree in geographic information system from Xi'an University of Science and Technology, Xi'an, China, in 2004, the M.Sc. degree in cartography and geographic information system from Central South University, Changsha, China, in 2007, and the Ph.D. degree in cartography and geographic information system from the Institute of Remote Sensing Applications, Chinese Academy of Science, Beijing, China, in 2010.

He is currently an Assistant Researcher with the State Key Laboratory of Remote Sensing Science, Institute of Remote Sensing and Digital Earth, Chinese Academy of Sciences, Beijing, China. His research interests focus on the retrieval and validation of land surface temperature/emissivity from satellite data.

Qinhuo Liu received the B.Sc. degree in hydrogeology and engineering geology from Southwest Jiaotong University, Chengdu, China, in 1988, and the M.Sc. degree in cartography and remote sensing and Ph.D. degree in atmospheric physics from Peking University, Beijing, China, in 1994 and 1997, respectively.

He was with INRA of France in 1998, Boston University in 1999, the University of Maryland in 2004, and George Mason University in 2010 as a Visiting Scholar. He has been with the Institute of Remote Sensing Applications, Chinese Academy of Sciences, Beijing, China, from 1997. He is currently a Professor, Deputy Director of the State Key Laboratory of Remote Sensing Science, Institute of Remote Sensing and Digital Earth, Chinese Academy of Sciences, Beijing. His research interests include radiation transfer modeling, quantitative remote sensing inversion, assimilation, and applications.

Yongming Du received the B.Sc. degree in geography from Yantai Normal College, Yantai, China, in 1999, the M.Sc. degree in cartography and remote sensing from Peking University, Beijing, China, in 2003, and the Ph.D. degree in cartography and remote sensing from the Institute of Remote Sensing Applications, Chinese Academy of Sciences, Beijing, in 2006.

He is currently an Associate Research Fellow with the State Key Laboratory of Remote Sensing Science, Institute of Remote Sensing and Digital Earth, Chinese Academy of Sciences, Beijing, China. His research interests focus on the radiation transfer model of vegetation canopy.

Jinxiong Jiang is currently working toward the Ph.D. degree in cartography and geographic information system at State Key Laboratory of Remote Sensing Science, Institute of Remote Sensing and Digital Earth, Chinese Academy of Sciences, Beijing, China.

Her current research interests focus on the retrieval of emissivity and surface temperature from satellite data.

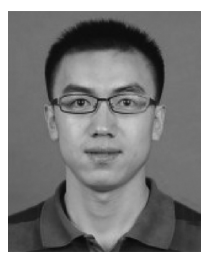

Heshun Wang received the B.Sc. degree in geographic information system from Jilin University, Changchun, China, in 2008, and the M.A. degree in cartography and geographic information system from Beijing Research Institute of Uranium Geology, Beijing, China, in 2011. He is currently working toward the Ph.D. degree in cartography and geographic information system at State Key Laboratory of Remote Sensing Science, Institute of Remote Sensing and Digital Earth, Chinese Academy of Sciences, Beijing, China.

His main research interests focus on land surface emissivity measurement, inversion, and modeling.